ACCEPTED VERSION

Mohammad Babazadeh, Paul L. Burn and David M. Huang
Calculating transition dipole moments of phosphorescent emitters for efficient organic light-emitting diodes
Physical Chemistry Chemical Physics, 2019; 21(19):9740-9746

Published at: http://dx.doi.org/10.1039/c9cp01045a

Journal Name

ARTICLE TYPE

Cite this: DOI: 10.1039/xxxxxxxxxx

Calculating transition dipole moments of phosphorescent emitters for efficient organic light-emitting diodes†

Mohammad Babazadeh,[a] Paul L. Burn,*[a] and David M. Huang*[b]

Received Date
Accepted Date

DOI: 10.1039/xxxxxxxxxx

www.rsc.org/journalname

The out-coupling of light from an organic light-emitting diode, and thus its efficiency, strongly depends on the orientation of the transition dipole moment (TDM) of the emitting molecules with respect to the substrate surface. Despite the importance of this quantity, theoretical investigations of the direction of the TDM of phosphorescent emitters based on iridium(III) complexes remain limited. One challenge is to find an appropriate level of theory able to accurately predict the direction of the TDM. Here, we report relativistic time-dependent density functional theory (TDDFT) calculations of the TDM, emission energies and lifetimes for both the ground-state (S_0) and triplet (T_1) excited-state geometries of *fac*-tris(2-phenylpyridyl)iridium(III) (Ir(ppy)$_3$), using the two-component zero-order regular approximation (ZORA) or including spin-orbit coupling (SOC) perturbatively using the simpler one-component (scalar) formulation. We show that the one- and two-component approaches give similar emission energies and overall radiative lifetimes for each individual geometry. Use of the S_0 geometry leads to two of the excited triplet substates being degenerate, with the degeneracy lifted for the T_1 geometry, with the latter matching experiment. Two-component calculations using the T_1 geometry give results for the direction of the TDM more consistent with experiment than calculations using the S_0 geometry. Finally, we show that adding a dielectric medium does not affect the direction of TDM significantly, but leads to better agreement with the experimentally measured radiative lifetime.

1 Introduction

Organic light-emitting diodes (OLEDs) represent an important shift in display and solid-state lighting technologies.[1] Improving the internal quantum efficiency from only a few percent in early fluorescent thin-film devices[2] to the theoretical limit of 100% for phosphorescent emitters has provided the impetus for the commercialization of devices based on OLEDs.[3] OLEDs offer a number of advantages compared to other emissive device technologies, including flexible form factor, ultra-thin devices, and even semi-transparency. A limiting factor that strongly affects the external quantum efficiency of OLEDs is light loss due to poor out-coupling from the devices.[4,5] The emissive layer in many of the most efficient OLEDs is composed of an emissive phosphorescent organometallic guest doped into a semiconducting organic host matrix. Radiation from an oscillating dipole is strongest perpendicular to its axis. Thus, these guests emit light perpendicular to their transition dipole moment (TDM) vectors. As a consequence, the out-coupling efficiency is strongly enhanced when the TDMs are aligned parallel to the OLED substrate surface.[6] Therefore, to determine the exact orientation of the TDM of a particular emitter in a host–guest system, it is necessary to know how the molecule is aligned with respect to the substrate[7,8] and how the TDM is oriented with respect to the molecular frame of the emitter. There are only a few reports of phosphorescent systems for which the spatial orientation of the TDM with respect to the molecular frame has been verified experimentally.[9,10] For example, Steiner et al. used single-molecule spectroscopy to show large fluctuations in the TDM direction of iridium(III)-based phosphorescent complexes with time, which were attributed spontaneous breaking of the C_3 symmetric structure of the complexes in the excited state.[10] In the absence of experimental data, quantum-chemistry calculations based on time-dependent density functional theory

[a] *Centre for Organic Photonics & Electronics, School of Chemistry and Molecular Biosciences, The University of Queensland, Queensland, 4072 Australia. Fax: +61 (07)33469273; Tel: +61 (0)733467614; E-mail: p.burn2@uq.edu.au*

[b] *Department of Chemistry, School of Physical Sciences, The University of Adelaide, Adelaide 5005, Australia. E-mail: david.huang@adelaide.edu.au*

† Electronic Supplementary Information (ESI) available: Gas-phase and dielectric medium DFT and TDDFT input files and molecular geometries, structural parameters of the B3LYP-optimized geometries, structural parameters of T_1 of the UDFT/BP86-optimized geometries in *vacuo* and in a dielectric medium, emission energies and radiative lifetimes of the triplet state calculated for different geometries using B3LYP and BP86 functionals, and degree of charge transfer in the emission process based on the S_0 geometry. See DOI:

(TDDFT) can be an invaluable tool for determining the direction of the TDM of emissive materials. For spin-allowed transitions, the TDM can be accurately calculated without spin-orbit coupling (SOC). However, for phosphorescent materials such as those based on iridium(III) complexes, emission from the excited triplet states to the singlet ground state relies on SOC and hence determination of the TDMs and optical properties needs to take into account SOC. *Fac*-tris(2-phenylpyridyl)iridium(III), shown in Figure 1, is the archetypical phosphorescent emitter, which has been used in highly efficient OLEDs. Given the experimental data available [11,12] it has proven a useful compound for exploring theoretical methods [13] for understanding the the optical and structural properties of phosphorescent complexes.

Several methods have been developed to include SOC in TDDFT calculations. [14–16] Among these methods, perturbative one-component scalar-relativistic TDDFT calculations with the zero-order regular approximation (ZORA) to the Dirac equation (pSOC-TDDFT) [17] has been reported to give essentially the same results for the optical properties (emission energies and excited state lifetimes) as those obtained from the more expensive non-perturbative two-component ZORA TDDFT (SOC-TDDFT) calculations. [18] In particular, Jansson et al. [19] have reported that pSOC-TDDFT gives good agreement with SOC-TDDFT for the radiative decay rates of phosphorescent emitters. However, one difference between different studies has been the geometry used to determine the photophysical properties. In some cases, the optimized singlet ground-state (S_0) geometry [16] has been used while other studies have reported emissive properties calculated using the optimized triplet (T_1) geometry correlate better with experiment. [20,21] Gonzalez-Vazquez et al. [22] recently reported that when pSOC-TDDFT calculations are used the optical properties of *fac*-Ir(ppy)$_3$ change as the geometry transitions from the ground state (S_0) to the excited triplet (T_1) geometry. In addition, most calculations of the optical properties of such complexes have been undertaken in *vacuo* and have not taken into account the dielectric properties of the host medium that is typically used in devices. Although recent studies have accurately matched the experimentally measured emission energies and radiative lifetimes of iridium(III) complexes, computational studies on the orientation of the TDM have been limited. [23,24] In the case of Ir(ppy)$_3$, computational results for the direction of TDM have not been consistent. [23–25] However, determining the source of these discrepancies is difficult, since in some cases the methodology used to determine the TDM has not been adequately described.

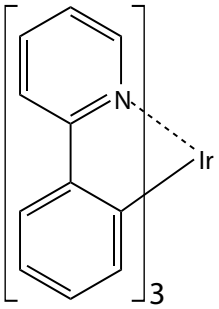

Fig. 1 Chemical structure of Ir(ppy)$_3$

In this work we describe a computational approach for predicting the direction of the TDM and emission properties of phosphorescent complexes, with Ir(ppy)$_3$ used as an exemplar. We determine the optimized ground-state (S_0) and first excited triplet-state (T_1) geometries of Ir(ppy)$_3$ and then compare the optical properties of the complex for both the S_0 and T_1 geometries using pSOC-TDDFT and SOC-TDDFT, including the role of the molecular geometry on the TDM direction. Finally, we report how the emission energies and radiative lifetimes are affected by the environment by using an implicit dielectric continuum model.

2 Computational methods

The SOC effect plays two important roles in phosphorescence from complexes such as Ir(ppy)$_3$. First, SOC enables fast intersystem crossing from an excited singlet state ($S_n, n > 0$) to the first excited triplet state (T_1), a process known as triplet harvesting. [26] Second, it activates emission from the excited triplet state to the singlet ground state, which is a formally spin-forbidden transition. [27] Previous theoretical studies on the optical properties of phosphorescent complexes have included SOC in the their calculations. [13,15,28]

The SOC effect splits the T_1 state into three substates ($T_{1,1}$, $T_{1,2}$, and $T_{1,3}$) that are separated in energy in the absence of an external magnetic field. This effect is known as the zero-field splitting (ZFS). [27] The radiative decay rate from triplet substate $T_{1,i}$ is given by [29]

$$k_{\mathrm{r},i} = k_{\mathrm{r}}(\mathrm{S}_0, \mathrm{T}_{1,i}) = \frac{4\alpha_0^3}{3t_0} \Delta E^3_{\mathrm{S}_0-\mathrm{T}_{1,i}} \sum_{j\in\{x,y,z\}} |M_j^i|^2 \qquad (1)$$

where $\Delta E_{S_0-T_{1,i}}$ is the transition energy, M_j^i is the transition moment, α_0 is the fine structure constant, and $t_0 = (4\pi\varepsilon_0)^2\hbar^3/m_e e^4$, where ε_0 is the permittivity of free space, $\hbar$ is the reduced Planck's constant, and m_e and e are the rest mass of the electron and the elementary charge, respectively. Assuming that the thermal population of the three substates is given by Boltzmann distribution, the overall radiative decay rate is

$$k_{\mathrm{r}} = \frac{k_{\mathrm{r},1} + k_{\mathrm{r},2}\exp(-\Delta E_{\mathrm{ZFS}_{1,2}}/k_{\mathrm{B}}T) + k_{\mathrm{r},3}\exp(-\Delta E_{\mathrm{ZFS}_{1,3}}/k_{\mathrm{B}}T)}{1 + \exp(-\Delta E_{\mathrm{ZFS}_{1,2}}/k_{\mathrm{B}}T) + \exp(-\Delta E_{\mathrm{ZFS}_{1,3}}/k_{\mathrm{B}}T)} \qquad (2)$$

where $\Delta E_{\mathrm{ZFS}_{i,j}}$ is the zero-field splitting between substates i and j, which is typically less than 200 cm^{-1} for phosphorescent emitters. [26] In this case, $\Delta E_{\mathrm{ZFS}_{i,j}} < k_{\mathrm{B}}T$ and eqn (2) can be approximated as

$$k_{\mathrm{r}} \approx \frac{1}{3}\left(k_{\mathrm{r},1} + k_{\mathrm{r},2} + k_{\mathrm{r},3}\right) \qquad (3)$$

As the radiative lifetime is the inverse of the radiative decay rate, the overall radiative lifetime is then given by

$$\frac{1}{\tau_{\mathrm{rad}}} \approx \frac{1}{3}\left(\frac{1}{\tau_1} + \frac{1}{\tau_2} + \frac{1}{\tau_3}\right) \qquad (4)$$

where $\tau_i = 1/k_{\mathrm{r},i}$. The validity of this approximation has been previously verified. [29]

In the calculations here, the ground-state geometry of Ir(ppy)$_3$

was optimized using the generalized-gradient approximation (GGA) BP86 functional and the TZ2P Slater type basis set. Starting from the optimized geometry of the ground state, the geometry of the excited triplet state of $Ir(ppy)_3$ was then optimized using the TDDFT excited-state geometry optimization approach with the same level of theory. For comparison, the geometries were also optimized using the B3LYP functional and the TZ2P Slater-type basis set, with results given in the ESI (Table S1).

Following geometry optimization, the emission energies and radiative lifetimes of $Ir(ppy)_3$ were determined using pSOC-TDDFT and SOC-TDDFT calculations for both the S_0 and T_1 state geometries. For the pSOC-TDDFT calculations the 20 lowest scalar relativistic singlet and triplet excitations were used. It should be noted that although in principle phosphorescent emission at room temperature can occur from any of the three substates of T_1, each substate has a different oscillator strength. As a consequence, it is often the case that a transition from one of the substates to the ground state will have an oscillator strength that is orders of magnitude larger than the other two and, thus, dictates the emission properties.[30] SOC-TDDFT calculations were used to calculate the TDM direction associated with the transition of the substate of T_1 to the ground state that had the largest oscillator strength.

Finally, the effect of the host matrix (in this case the commonly used host material 4,4′-bis(*N*-carbazolyl)biphenyl (CBP)) on the emissive properties of the $Ir(ppy)_3$ molecules were included using the conductor-like screening model (COSMO) to describe the host as a dielectric continuum with the dielectric constant of CBP (which has an experimentally measured static dielectric constant $\varepsilon = 3.5$ and optical dielectric constant $\varepsilon_{opt} = n^2 = 3.2$, where n is the refractive index). The implementation of the dielectric continuum in the TDDFT calculations was a linear-response (LR) approach. The non-equilibrium formalism was used for the calculations of the emission energies using the static and optical dielectric constants while the solvent-relaxed formalism used the static dielectric constant for the excited-state geometry optimizations. The role of excited-state solvent equilibration was also studied by conducting spin-unrestricted DFT (UDFT) calculations in the dielectric medium. in this case, the excited triplet (T1) state of $Ir(ppy)_3$ was optimized using the UDFT/BP86/TZ2P level of theory in the gas phase and in the dielectric medium. The energy difference between the singlet ground and excited triplet states of the complex was then calculated using UDFT/B3LYP/TZP in *vacuo* and in the dielectric medium.

All pSOC-TDDFT and SOC-TDDFT calculations, both in *vacuo* and in the dielectric medium, were done using the TZP Slater type basis set and B3LYP functional. The emission energies and radiative lifetimes for each T_1 substate were also calculated using the BP86 functional with the same basis set (see ESI Table S3).

All calculations were performed using the Amsterdam Density Functional package (ADF 2017.103).[31]

3 Results and discussion

3.1 In *vacuo*

3.1.1 Structures and optical properties

The employed geometry is critical to accurately predict the optical properties of iridium(III) complexes. As phosphorescent emission occurs from the excited triplet state (T_1) to the ground state (S_0), the structures of S_0 and T_1 of the iridium(III) emitter need to be optimized. The Ir–N, Ir–C bond lengths for the optimized geometries of $Ir(ppy)_3$ are summarized in Table 1.

Table 1 Selected bond lengths of $Ir(ppy)_3$ (in Å) in the S_0 and T_1 optimized geometries at the BP86/TZ2P level of theory

	S_0	T_1	(S_0-T_1)
Ir–N1	2.151	2.195	-0.044
Ir–N2	2.151	2.163	-0.012
Ir–N3	2.151	2.156	-0.005
Ir–C1	2.024	2.029	-0.005
Ir–C2	2.024	1.980	0.044
Ir–C3	2.024	2.048	-0.024

The optimized structures of the ground state and excited triplet state of $Ir(ppy)_3$ are in a good agreement with the optimized geometries reported by Gonzalez-Vazquez et al.[22] It is clear that ground-state structure has C_3 symmetry, with the symmetry broken in the triplet geometry. Breaking of the symmetry in the excited triplet state for $Ir(ppy)_3$ has been reported previously.[32,33] Steiner et al.[10] have also demonstrated experimentally using single-molecule spectroscopy that the C_3 the complex undergoes spontaneous symmetry breaking in the first excited triplet state.

Table 2 compares the calculated emission energies and radiative lifetimes of the three excited triplet substates using the pSOC-TDDFT and SOC-TDDFT approaches. The calculated emission energy of each substate is essentially the same (within 0.03 eV) for both geometries using the two approaches. The two methods give lifetimes of the same order of magnitude for each substate for the S_0 geometry, but produce some discrepancy for the substate of intermediate lifetime for the T_1 geometry. Importantly, the substate with the largest oscillator strength has a similar lifetime independent of the TDDFT method used. The optical properties calculated in the S_0 geometry show that the second and third spin-orbit coupled excitations (substates) are approximately degenerate and have shorter lifetimes than the lowest excited substate, which is almost dark (longer lifetime). On the other hand, the substates in the T_1 geometry are non-degenerate and lower in energy. In contrast to the S_0 geometry, in which two substates have equal lifetimes, the relative lifetimes in the T_1 geometry ($\tau_{1,1}$=1600 μs, $\tau_{1,2}$=12 μs and $\tau_{1,3}$=3.3 μs using pSOC-TDDFT) follow the trend of the experimentally measured values ($\tau_{1,1}$=116 μs, $\tau_{1,2}$=6.4 μs and $\tau_{1,3}$=0.2 μs).[11]

3.1.2 Transition dipole moment

Previously reported results using TDDFT calculations (albeit using different functionals and basis sets) by Moon et al. for $Ir(ppy)_3$ and by Morgenstern el al. have found the TDM vector to lie at an angle of 45°[24] and between 35° and 38° to the Ir–N bond[25], respectively. From a full relativistic SOC-TDDFT calcu-

Table 2 Comparison of transition energies and lifetimes calculated for S_0 and T_1 structures using pSOC-TDDFT and SOC-TDDFT approaches

	S_0				T_1			
	pSOC-TDDFT		SOC-TDDFT		pSOC-TDDFT		SOC-TDDFT	
substate	E/eV	τ/s	E/eV	τ/s	E/eV	τ/s	E/eV	τ/s
$T_{1,1}$	2.500	0.432×10^{-3}	2.466	0.176×10^{-2}	2.000	0.160×10^{-2}	1.973	0.270×10^{-3}
$T_{1,2}$	2.506	0.224×10^{-5}	2.477	0.317×10^{-5}	2.001	0.120×10^{-4}	1.977	0.201×10^{-2}
$T_{1,3}$	2.507	0.214×10^{-5}	2.478	0.300×10^{-5}	2.015	0.330×10^{-5}	1.997	0.486×10^{-5}

lation using the optimized T_1 geometry, we found that the TDM vector for substate $T_{1,3}$ (the substate with shortest emissive lifetime in the T_1 state) lies in the C–Ir–N plane at an angle of 9° to the Ir–N bond as shown in Figure 2. This value is more consistent with the 0° angle deduced from a combination of experiment and molecular dynamics simulations[8] than the previously calculated values.

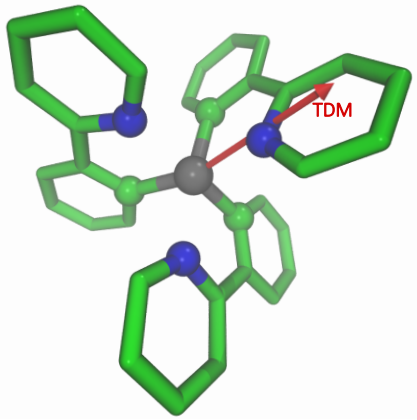

Fig. 2 Direction of TDM vector for $Ir(ppy)_3$ calculated using SOC-TDDFT calculation. The C_3 symmetry axis of the molecule lies perpendicular to plane of the page.(Note that the molecule has lower than C_3 symmetry in the T_1 state.)

A possible cause of the discrepancy between the previously published results and ours is the choice of geometry (e.g., S_0 vs T_1) in the TDDFT calculations. While we used the optimized T_1 geometry, the choice of geometry in refs. 24 and 25 is not specified. To investigate the effect of changing the $Ir(ppy)_3$ geometry on the direction of the TDM, we performed SOC-TDDFT calculations for a range of geometries that were linearly extrapolated between the optimized ground singlet state and excited triplet state geometries. 0% corresponds to the ground-state S_0 geometry and 100% indicates the excited triplet-state T_1 geometry. Thus, for example, the 50% geometry corresponds to a structure in which all atoms are at the midpoints between their positions in the S_0 and T_1 geometries. This method was previously used by Gonzalez-Vazquez et al.[22] to study the ZFS of *fac*-$Ir(ppy)_3$ in the ground state (S_0), lowest energy triplet (T_1), and at intermediate geometries. The calculated angle between the TDM and Ir–N bond at intermediate geometries is shown in Figure 3 and, in all cases, the TDM corresponds to the transition from the $T_{1,3}$ substate to the S_0 ground state.

The calculated TDMs for all the geometries are in the plane of the 2-phenylpyridine ligand and it is clear that the angle between

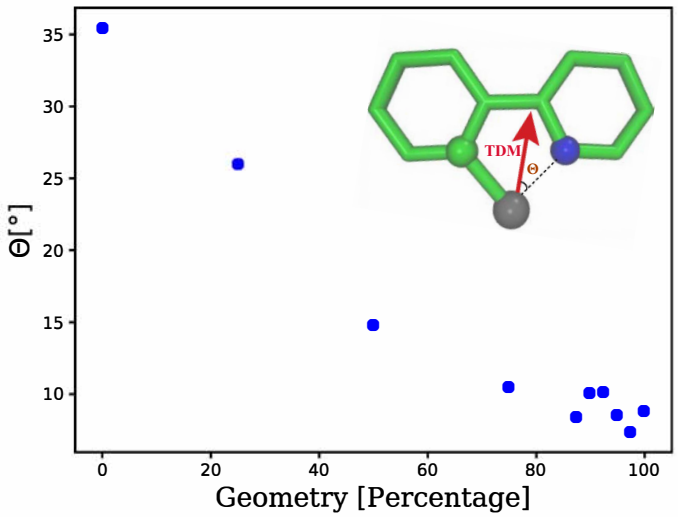

Fig. 3 Direction of TDM vector relative to Ir–N bond as *fac*-$Ir(ppy)_3$ changes from the S_0 to the T_1 geometries

the TDM and Ir–N bond decreases almost monotonically from 35° to 9° in changing from the S_0 to the T_1 geometry. It is reasonable to expect the TDM calculated using the T_1 geometry will match the experimental results as emission occurs from the T_1 state while the molecule is in the T_1 geometry. Our findings that both the TDM and radiative lifetimes, which are related through eqn (1), calculated for the T_1 geometry match experiment better than those calculated for the S_0 geometry confirm these expectations. A final feature of the TDM calculations using full SOC-TDDFT is that the TDM is towards the ligand that has the shortest bonds to the iridium atom in the excited triplet-state geometry. However, it should be noted that these calculations do not specify which of the Ir–N bonds the TDM will point along, with any one of the three ligands being equally likely to become the one with the shortest bonds to the iridium atom in an isotropic environment. Selection of the particular direction could arise from spontaneous symmetry breaking associated with thermally activated molecular vibrations. Indeed, Steiner et al.[10] have demonstrated using single-molecule spectroscopy that the TDM of a related Ir complex with C_3 symmetry undergoes spontaneous fluctuations in direction over time.

We also performed SOC-TDDFT calculations using the BP86 functional on the S_0 and T_1 structures to calculate the TDM. Consistent with the B3LYP results, the angle between the TDM and Ir–N bond was found to decrease (from 30° and 16°, respectively) in going from the S_0 to the T_1 geometry. It should be noted that

using pSOC-TDDFT within the ADF suite does not allow output of the TDM with spin-orbit coupling. The consequence of the lack of spin-orbit coupling in the output is that there is a large angle between the TDM and Ir–N bond calculated from the transition density using this approach.[8]

3.1.3 Excited-state charge transfer

To clarify the physical origin of the direction of the TDM of $Ir(ppy)_3$, we calculated the charge transfer that occurs during the transition between the T_1 and S_0 states using the methodology proposed by Joo et al.[34] The method defines the degree of charge transfer using only electron densities in the highest energy occupied Kohn-Sham (KS) orbitals instead of using the total electron density. This was found to yield degrees of charge transfer that were independent of the charge analysis method for a variety of systems.[34] The number of occupied orbitals required to describe the charge-transfer process, which is called the "active space", is determined as the minimum number of electrons (orbitals) at which the degree of charge transfer (charge in the ground state minus charge in the excited state) approximately converges. Mulliken charges in the S_0 and T_1 states were calculated using single-point DFT calculations for the S_0 and T_1 geometries. The active space was determined by incremental inclusion of lower energy orbitals until the degree of charge transfer converged. Figure 4 shows the calculated degree of charge transfer on the iridium atom and the three 2-phenylpyridine ligands.

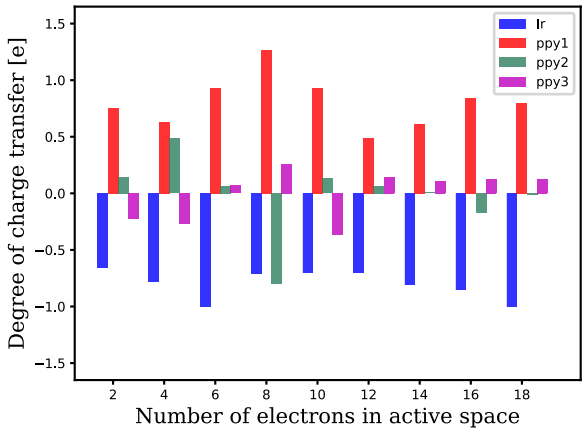

Fig. 4 Degree of charge transfer for emission process (charge in ground state minus charge in excited state) in $Ir(ppy)_3$ on the iridium atom and the three ligands as a function of number of electrons in the active space

From Figure 4 it can be seen that the degree of charge transfer converges when between 12 and 18 electrons are included. Importantly, the results show that during the emission process, most of the charge is transfered from one of the ligands to the iridium(III) atom. The ligand from which the charge is transferred is the one that has the shortest Ir–N bond. Thus, the results from the charge transfer calculation are consistent with those of the TDM calculations, which show the TDM vector pointing approximately along the Ir–N bond of the ligand with the shortest Ir–N bond to the iridium(III) atom. The calculation also shows that using the S_0 geometry gives equal charge transfer to all the ligands (see ESI Fig. S1), which is inconsistent with the experimental work of Steiner et al. that shows that emission involves a single ligand.[10]

3.2 Dielectric continuum

Given that phosphorescent emitters are normally blended with a host material, in the final part of the study we investigated the effect of the host dielectric constant on the optical properties of $Ir(ppy)_3$. To do this we first determined whether the static dielectric constant affected the S_0 and T_1 state geometries by comparing those calculated *in vacuo* and for a static dielectric constant of 3.5, which is the experimentally measured dielectric constant of CBP. The optimized geometries were found to be essentially the same and hence the subsequent calculations were performed using the geometries optimized *in vacuo*.

It would be expected that different hosts would have different dielectric constants. We therefore varied the static dielectric constant from $\varepsilon = 1$ to $\varepsilon = 5$ and calculated the optical properties of the $Ir(ppy)_3$ using the optimized T_1 geometry and pSOC-TDDFT incorporating the 20 lowest scalar relativistic singlet and triplet excitations. Figure 5 shows the emission energies of the three substates of T_1 and Figure 6 the radiative lifetime of the $T_{1,3}$ substate, which has the shortest lifetime, versus the static dielectric constant of the medium. It can be seen that moving from vacuum to the dielectric medium (host) the emission energies of all three substates of T_1 increase and the lifetime of the emissive $T_{1,3}$ substate decreases.

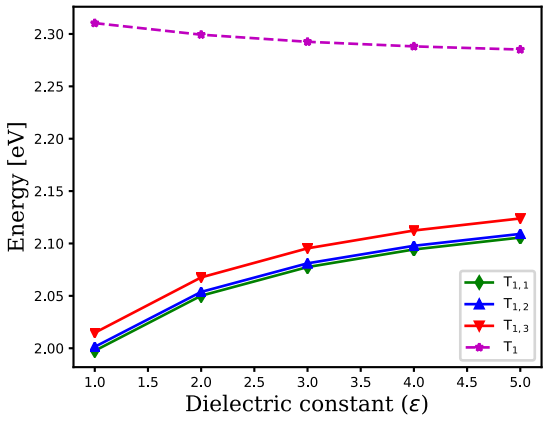

Fig. 5 Emission energies of the three substates of T_1 (solid lines) in different static dielectric constants calculated using pSOC-TDDFT calculation in a dielectric medium. The calculated energy difference between the excited triplet state (T_1) and ground S_0 state in the T_1 geometry calculated using UDFT is shown for comparison (dashed line)

Furthermore, we compared the emission properties of $Ir(ppy)_3$ *in vacuo* and with the static and optical dielectric constants of CBP, $\varepsilon = 3.5$ and $\varepsilon_{opt} = n^2 = 3.2$, respectively (Table 3). Including the dielectric medium in the pSOC-TDDFT calculation, the radiative lifetime of $T_{1,3}$ significantly decreases to around $1.5\,\mu s$ compared to $3.3\,\mu s$ *in vacuo*. Using eqn (4), the overall radiative

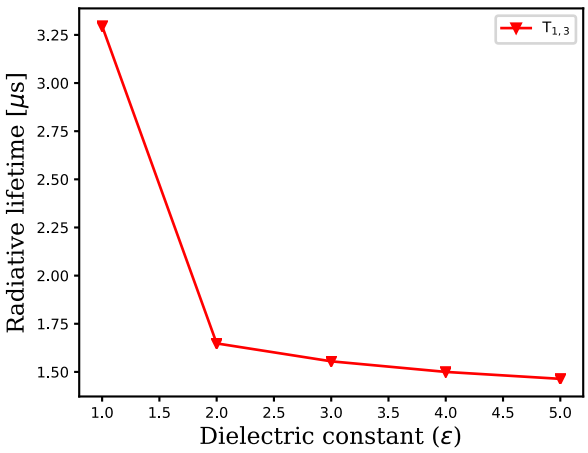

Fig. 6 Radiative lifetime of substate $T_{1,3}$ (with the shortest lifetime) as a function of static dielectric constant of dielectric medium

Table 3 Comparison of emission energies and radiative lifetimes of substates of T_1 in *vacuo* and in the dielectric medium ($\varepsilon = 3.5, \varepsilon_{opt} = 3.2$)

	in *vacuo*		dielectric medium	
substate	E/eV	τ/s	E/eV	τ/s
$T_{1,1}$	2.000	0.160×10^{-2}	2.078	0.820×10^{-3}
$T_{1,2}$	2.001	0.120×10^{-4}	2.081	0.112×10^{-4}
$T_{1,3}$	2.015	0.330×10^{-5}	2.095	0.156×10^{-5}

lifetime of $Ir(ppy)_3$ in CBP is estimated to be about τ_{rad} =4.1 μs. Thus, the polarization effect of the dielectric medium shortens the overall radiative lifetime, with the calculated lifetime more consistent with the experimentally measured value (1.6 μs measured in CH_2Cl_2 [11]). (Note CH_2Cl_2 has a static dielectric constant of 8.9 but Figure 6 shows that the lifetime does not vary significantly when the static dielectric constant is greater than 2). *In vacuo*, the total radiative lifetime is estimated to be 7.8 μs.

We also considered the effect of dielectric medium on the direction of the TDM. Using SOC-TDDFT we found that the dielectric medium does not effect the angle of the TDM with respect to the Ir–N bond significantly, with the TDM being found between 9° and 11°.

The dielectric medium would be expected to stabilize the excited triplet state of $Ir(ppy)_3$ given that it has charge-transfer character, which would reduce the emission energy in contrast to the small increase in energy observed for the TDDFT calculations in Figure 5. At first sight, this suggests that the linear-response TDDFT solvation model may not be adequate for treating excited-state solvation in $Ir(ppy)_3$, since solvent relaxation as the electrostatic potential changes between the ground and excited state is not taken into accounted in such a model.[35] This problem has recently been shown for a number of organic thermally activated delayed fluorescence (TADF) emitters.[36] To investigate the potential role of solvent relaxation on the excited T_1 state of $Ir(ppy)_3$ we carried out spin-unrestricted DFT (UDFT) calculations in the dielectric medium with the excited triplet state of $Ir(ppy)_3$ optimized using UDFT *in vacuo* and in the dielectric medium. It was found that the structure of the excited triplet state did not change significantly when moving from vacuum to the dielectric medium (see ESI Table S2). Using the gas phase optimized structure of T_1 we next determined the energy difference between the singlet ground and excited triplet states of the complex using UDFT in the dielectric medium, which is shown as the dashed line in Figure 5. It can be seen that as the static dielectric constant of the medium is varied between $\varepsilon = 1$ and $\varepsilon = 5$ the solvent field does stabilize the excited T_1 state relative to the ground S_0 state, although the stabilization is very small ($\sim$ 20 meV). To rationalize this result, we calculated the permanent dipole moment of $Ir(ppy)_3$ in the S_0 and T_1 states from the UDFT calculation, and found them to be very similar, at 6.2 D and 6.4 D. The similarity in the permanent dipole between the S_0 and T_1 states of $Ir(ppy)_3$ are in significant contrast to the TADF emitters studied by Mewes, which showed much larger changes in dipole moment between the ground and excited states and hence solvent stabilization. Therefore, in the cases where the ground and excited state permanent dipoles are similar, the linear-response approach to the excited-state solvation can regarded as a reasonable approximation.

4 Conclusions

We have calculated the optical properties of $Ir(ppy)_3$ using ground singlet-state and excited triplet-state geometries. The calculations indicate the symmetric singlet ground-state geometry of $Ir(ppy)_3$ is broken upon going to the first excited triplet state. We showed that the computationally efficient pSOC-TDDFT approach gives similar results for emission energies and the overall radiative lifetime to the more accurate full SOC-TDDFT approach. We also found that the direction of the TDM determined from the full SOC-TDFT calculations with the excited triplet-state geometry matches experiment more closely than the TDM from analogous calculations using the singlet ground-state geometry. We also confirmed that the direction of the transition dipole moment is related to the metal-to-ligand charge transfer that occurs in the emission process. Furthermore, we found that using either the BP86 or the B3LYP functional as representatives of broad class of commonly employed methods (generalized gradient approximation and hybrid) gives qualitatively similar results for emission energies, radiative lifetimes, and the direction of TDM. It should be noted that conventional GGA and global hybrid functionals often do not describe charge-transfer excited states well,[37] in particular underestimating transition energies, as observed here. Improved accuracy could potentially be achieved with a range-separated hybrid functional. Finally, we demonstrate hat adding a dielectric medium to include the effect of the host matrix does not affect the TDM direction significantly but gives the radiative lifetime close to experimental results.

Conflicts of interest

There are no conflicts to declare.

Acknowledgements

P.L.B. is an ARC Laureate Fellow (FL160100067) and the work was supported by this Fellowship. This work utilised the computational resources provided by the Australian Government through

the National Computational Infrastructure under the National Computational Merit Allocation Scheme.

Notes and references

1 S. R. Forrest, *Nature*, 2004, **428**, 911–918.

2 C. W. Tang and S. A. VanSlyke, *Appl. Phys. Lett.*, 1987, **51**, 913–915.

3 C. Adachi, M. A. Baldo, M. E. Thompson and S. R. Forrest, *J. Appl. Phys.*, 2001, **90**, 5048–5051.

4 S. Möller and S. Forrest, *J. Appl. Phys.*, 2002, **91**, 3324–3327.

5 T.-W. Koh, J.-M. Choi, S. Lee and S. Yoo, *Adv. Mater.*, 2010, **22**, 1849–1853.

6 M. J. Jurow, C. Mayr, T. D. Schmidt, T. Lampe, P. I. Djurovich, W. Brütting and M. E. Thompson, *Nat. Mater.*, 2016, **15**, 85–91.

7 C. Tonnelé, M. Stroet, B. Caron, A. J. Clulow, R. C. Nagiri, A. K. Malde, P. L. Burn, I. R. Gentle, A. E. Mark and B. J. Powell, *Angew. Chem. Int. Ed.*, 2017, **56**, 8402–8406.

8 T. Lee, B. Caron, M. Stroet, D. M. Huang, P. L. Burn and A. E. Mark, *Nano Lett.*, 2017, **17**, 6464–6468.

9 F. W. Vanhelmont, G. F. Strouse, H. U. Güdel, A. C. Stückl and H. W. Schmalle, *J. Phys. Chem. A*, 1997, **101**, 2946–2952.

10 F. Steiner, S. Bange, J. Vogelsang and J. M. Lupton, *J. Phys. Chem. Lett.*, 2015, **6**, 999–1004.

11 T. Hofbeck and H. Yersin, *Inorg. Chem.*, 2010, **49**, 9290–9299.

12 R. J. Berger, H.-G. Stammler, B. Neumann and N. W. Mitzel, *Eur. J. Inorg. Chem.*, 2010, **2010**, 1613–1617.

13 K. Nozaki, *J. Chin. Chem. Soc.*, 2006, **53**, 101–112.

14 P. J. Hay, *J. Phys. Chem. A*, 2002, **106**, 1634–1641.

15 A. R. Smith, P. L. Burn and B. J. Powell, *ChemPhysChem*, 2011, **12**, 2429–2438.

16 X. Li, B. Minaev, H. Ågren and H. Tian, *J. Phys. Chem. C*, 2011, **115**, 20724–20731.

17 F. Wang and T. Ziegler, *J. Chem. Phys.*, 2005, **123**, 154102.

18 F. Wang, T. Ziegler, E. van Lenthe, S. van Gisbergen and E. J. Baerends, *J. Chem. Phys.*, 2005, **122**, 204103.

19 E. Jansson, P. Norman, B. Minaev and H. Ågren, *J. Chem. Phys.*, 2006, **124**, 114106.

20 M.-X. Song, Z.-M. Hao, Z.-J. Wu, S.-Y. Song, L. Zhou, R.-P. Deng and H.-J. Zhang, *Int. J. Quantum Chem.*, 2013, **113**, 1641–1649.

21 F. De Angelis, L. Belpassi and S. Fantacci, *J. Mol. Struct. THEOCHEM*, 2009, **914**, 74–86.

22 J. P. Gonzalez-Vazquez, P. L. Burn and B. J. Powell, *Inorg. Chem.*, 2015, **54**, 10457–10461.

23 T. D. Schmidt, T. Lampe, P. I. Djurovich, M. E. Thompson, W. Brütting *et al.*, *Phys. Rev. Appl.*, 2017, **8**, 037001.

24 C.-K. Moon, K.-H. Kim and J.-J. Kim, *Nat. Commun.*, 2017, **8**, 791.

25 T. Morgenstern, M. Schmid, A. Hofmann, M. Bierling, L. Jäger and W. Brütting, *ACS Appl. Mater. Interfaces*, 2018, **10**, 31541–31551.

26 H. Yersin, A. F. Rausch, R. Czerwieniec, T. Hofbeck and T. Fischer, *Coord. Chem. Rev.*, 2011, **255**, 2622–2652.

27 A. F. Rausch, H. H. Homeier and H. Yersin, *Photophysics of Organometallics*, Springer, 2010, pp. 193–235.

28 B. Powell, *Coord. Chem. Rev.*, 2015, **295**, 46–79.

29 J. M. Younker and K. D. Dobbs, *J. Phys. Chem. C*, 2013, **117**, 25714–25723.

30 H. Yersin, *Highly efficient OLEDs with phosphorescent materials*, John Wiley & Sons, 2008.

31 G. t. Te Velde, F. M. Bickelhaupt, E. J. Baerends, C. Fonseca Guerra, S. J. van Gisbergen, J. G. Snijders and T. Ziegler, *J. Comput. Chem.*, 2001, **22**, 931–967.

32 K. Nozaki, *J. Chin. Chem. Soc.*, 2013, **53**, 101–112.

33 E. Jansson, B. Minaev, S. Schrader and H. Ågren, *Chem. Phys.*, 2007, **333**, 157–167.

34 B. Joo and E.-G. Kim, *Chem. Commun.*, 2015, **51**, 15071–15074.

35 J.-M. Mewes, J. M. Herbert and A. Dreuw, *Phys. Chem. Chem. Phys.*, 2017, **19**, 1644–1654.

36 J.-M. Mewes, *Phys. Chem. Chem. Phys.*, 2018, **20**, 12454–12469.

37 A. D. Laurent and D. Jacquemin, *Int. J. Quantum Chem.*, 2013, **113**, 2019–2039.